Journal of Applied Electrochemistry **33**: 1017–1024, 2003.

Anodic behaviour of arsenopyrite and cathodic reduction of ferrate(VI) and oxygen in alkaline solutions

M.J. NICOL[1],* and N. GURESIN[2]
[1]*A.J. Parker Cooperative Research Centre for Hydrometallurgy, Murdoch University, Murdoch, WA6150, Western Australia*
[2]*Department of Mining, Metals and Materials Engineering, University of Queensland, Brisbane, Queensland, Australia*
*(*author for correspondence, e-mail: M.Nicol@murdoch.edu.au)*

Received 8 July 2002; accepted in revised form 4 June 2003

Key words: alkaline oxidation, anodic oxidation, arsenopyrite, ferrate(VI), oxygen reduction

Abstract

This paper presents the results of an electrochemical study of the anodic characteristics of arsenopyrite in strongly alkaline solutions and of the cathodic reduction of ferrate(VI) and of dissolved oxygen at an arsenopyrite surface at potentials which are relevant to the oxidation reactions. Cyclic voltammetry at both arsenopyrite disc and arsenopyrite disc/platinum ring electrodes has shown that arsenic(III) is the main product of the anodic process at potentials in the region of the rest potential during oxidation by either ferrate(VI) or oxygen. Evidence for partial passivation of both the anodic and cathodic reactions has been obtained from potentiostatic current–time transients. The initial stage of oxidation by ferrate(VI) has been shown to be mass-transport controlled and this is also true of the oxidation by oxygen in dilute solutions of sodium hydroxide.

1. Introduction

The sulfide mineral arsenopyrite (FeAsS) is, like other arsenical sulfides and pyrite, a relatively common host mineral for gold. The correlation of arsenopyrite with gold has long been recognized and concentrations of up to 1.6 wt % gold in arsenopyrite have been recorded [1, 2]. Gold is recoverable by direct cyanidation if it exists as discrete grains between individual crystals of arsenopyrite. Gold in solid solution or as minute inclusions in arsenopyrite requires oxidation of the host mineral before cyanidation. This oxidation can be accomplished by either pyrometallurgical or hydrometallurgical techniques. Although arsenical concentrates have been treated by roasting for many years, the process is no longer environmentally acceptable due to the high levels of arsenic and sulfur dioxide in the roaster gases. Therefore, research has been focused on the development of aqueous oxidation processes the most commonly applied of which are pressure oxidation and bacterial oxidation each of which has its particular advantages and shortcomings. Thus, pressure oxidation requires autoclaves which are expensive to install, operate and maintain while the bio-oxidation process is slow and sensitive to operating conditions. Both of these processes produce acidic solutions which require neutralisation before recovery of gold by cyanidation.

There are several published reports [3–8] on the electrochemical oxidation of arsenopyrite in alkaline and acidic media which have focused on the overall electrochemical characteristics but have not dealt in detail with the nature of the products under various conditions of pH, temperature and potential. There are no reports of the cathodic characteristics of oxidants such as dissolved oxygen which could be used for the treatment of refractory gold concentrates containing arsenopyrite.

A previous study has shown that pyrite can be relatively rapidly oxidized by electrogenerated alkaline ferrate(VI) solutions [9]. This 'Ferrox process' offers an alternative to the above processes which could prove to be more economic, environmentally acceptable and compatible with downstream cyanidation processes which are required to operate in alkaline solutions.

Ferrate(VI) has not been studied in much detail as an oxidant because it is relatively unstable, particularly in acidic solutions. However, the above-mentioned study has confirmed that it can be produced with relatively high efficiencies by the anodic oxidation of high-carbon cast iron anodes in strongly alkaline solutions in which it is sufficiently stable to be used as an oxidant. The work has demonstrated that a cell of suitable design and materials of construction can be operated continuously and suitable operating conditions and monitoring procedures have been developed [9].

This approach has recently been extended to the oxidation of arsenopyrite and this paper is a report of an investigation of the electrochemical characteristics of anodic behaviour of arsenopyrite and of the cathodic reduction of ferrate(VI) and dissolved oxygen in strongly alkaline solutions. The objectives of this work have been to determine the rate determining steps in the overall oxidation process and to suggest possible mechanisms for the oxidation reactions.

2. Experimental details

A natural massive arsenopyrite mineral sample obtained from Hunnan Province, China was used to prepare rotating disc electrodes for the electrochemical studies. The sample was subjected to X-ray diffraction analysis using a Siemens X-ray diffractometer coupled to a Philips PW 1050 goniometer and a Sietronic SIE122 D automation system. No peaks other than those due to arsenopyrite could be detected. Elemental analysis of the sample by a Philips XL20 scanning electron microscope equipped with a Link ISIS energy-dispersive spectrometer confirmed that the sample contained only a minor (<1%) amount of other elements. Chemical analyses of the sample after complete dissolution was performed using ICP and AAS and the results showed 32.0% Fe, 51.9% As and 16.0% S with less than 0.1% of other impurities. The stoichiometry of the sample was calculated to be $Fe_{1.15}As_{1.39}S_{1.00}$.

Cylindrical rods (dia. 4.9 mm × 10.0 mm) were cut from the mineral sample by an ultrasonic mill. To construct rotating disc electrodes, the rods were attached to a stainless steel disc base by a conductive silver epoxy for solderless connections. The bars were then set in epoxy resin in cylindrical acrylic moulds. A conventional rotating disc assembly was used in electrochemical experiments and electrical contact between the detachable arsenopyrite electrodes and rotating shaft of the rotating disc assembly was achieved by means of an araldite resin encapsulated brass electrode holder. A similar procedure was followed to prepare a rotating ring disc electrode by using platinum tubing as ring. In this case the arsenopyrite bar was connected to a central rod and is insulated from platinum ring by PVC and epoxy resin. The calculated collection efficiency for the ring electrode was 0.30. Unless stated, all experiments were carried out at a rotation speed of 1000 rpm. Arsenopyrite electrodes were polished using P1200 grade silicon carbide water-proof paper and rinsed with water before each electrochemical experiment.

Electrochemical experiments were performed in a 100 mL capacity glass water-jacketed standard three-electrode electrochemical cell fitted with an entry port at the base for the Luggin capillary. A saturated calomel electrode and a Pt-wire electrode served as the reference and counter electrodes, respectively. Unless otherwise stated, all the experiments were preceded by bubbling ultrahigh purity nitrogen through the test solution and during these experiments nitrogen was used to provide a blanketing atmosphere. The test solution in the cell was thermostatted using a water bath and the bath temperature controlled at 20 °C. Deionized water from a Millipore Milli-Q system was used for the preparation of the solutions.

Sodium hydroxide solutions were prepared using reagent grade pellets. Ferrate(VI) solutions were prepared by anodic oxidation of a white cast iron anode in 40% sodium hydroxide solutions. The ferrate(VI) concentration was determined using the chromite method as described by Schreyer et al. [10].

A Princeton Applied Research (model 362) scanning potentiostat and a Bausch Lomb (model 2000) X–Y recorder were used to control the experiments and record the output respectively. All voltammograms were obtained using a sweep rate of 10 mV s^{-1}. All potentials are reported with respect to the saturated calomel reference electrode (SCE).

3. Results

3.1. *Rest potential measurements*

The rest potential of an arsenopyrite rotating disc electrode was measured as a function of time in 40% sodium hydroxide solutions containing various concentrations of ferrate(VI) and the results are given in Figure 1.

The rest potential varied with time in the range from −0.40 to −0.70 V depending on the concentration of the ferrate(VI) solution. As the concentration of the ferrate(VI) solution was decreased, the rest potential value shifted slightly to more negative values. The rest potential increased with time to a maximum value and then decreased gradually at the highest ferrate(VI) concentration used whereas it increased to a plateau value which was retained for at least one hour for the intermediate and lower ferrate(VI) concentrations. Similar rest potential behaviour has been observed for pyrite in ferrate(VI) solutions [3].

It was observed that a change in rotation speed of the electrode affected the rest potential of the system especially at low and intermediate ferrate(VI) concentrations. This behaviour can be seen in Figure 2. The rest potential shifted to more positive values when the rotation speed was increased from 100 to 1000 rpm indicating that the reaction of arsenopyrite with ferrate(VI) solution was at least partially controlled by diffusion.

The results of similar experiments in which the rest potential was measured in oxygenated alkaline solutions in the absence of ferrate(VI) are shown in Figure 3. Note the significant shift of the rest potential to more anodic potentials in the dilute solution.

3.2. *Cyclic voltammetry*

Before investigating the behaviour of arsenopyrite in ferrate(VI) solutions, some cyclic voltammogram studies were performed to establish the anodic characteristics

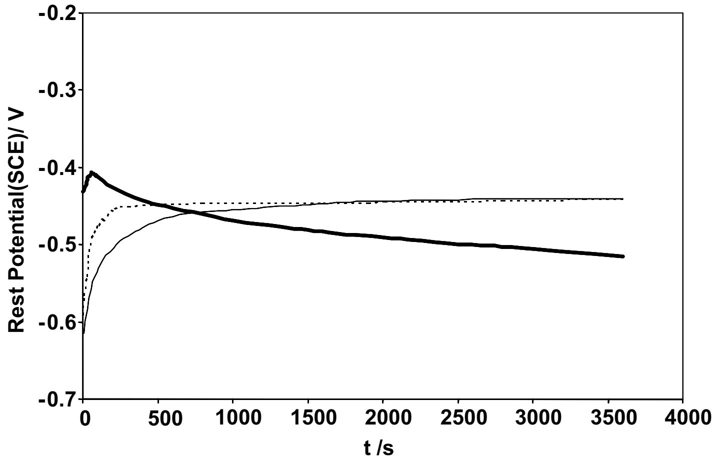

Fig. 1. Variation of the rest potential of arsenopyrite with time in ferrate(VI) solutions of different concentrations: (▬) 18.2, (—) 1.40 and (···) 5.10 mM.

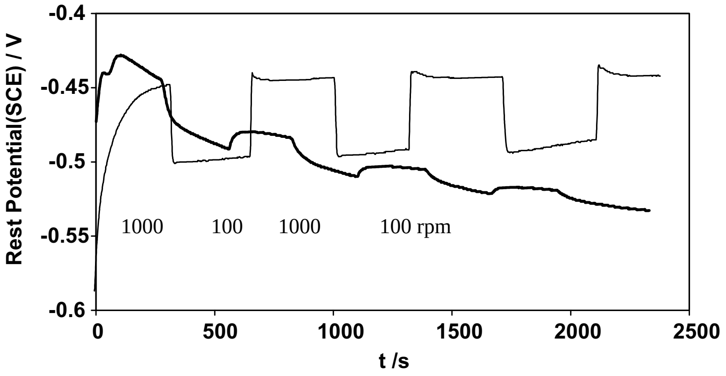

Fig. 2. Effect of rotation speed on rest potential of arsenopyrite in ferrate(VI) solutions of different concentrations: (—) 5.71 and (▬) 17.4 mM.

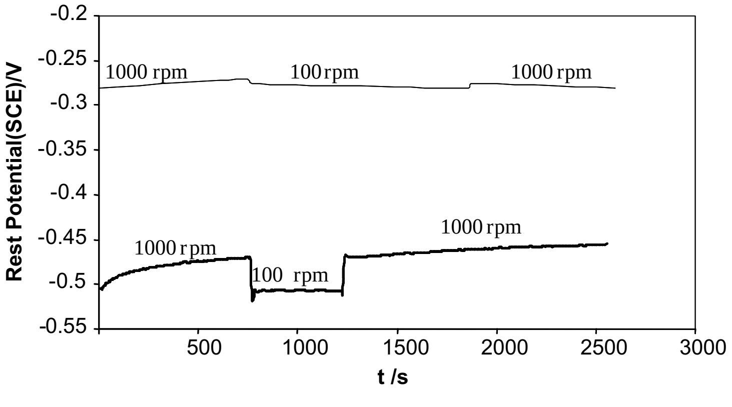

Fig. 3. Rest potential of arsenopyrite in oxygenated alkaline solutions of different concentrations: (▬) 20% NaOH and (—) 2% NaOH.

of arsenopyrite in concentrated sodium hydroxide solutions. Studies were focussed on the behaviour of the mineral in the potential region of −0.7 to −0.3 V which is relevant to the potentials experienced by the mineral under oxidation conditions. The results of voltammograms obtained in sodium hydroxide solutions of varying concentration in the absence of dissolved air are shown in Figure 4 (negative-going sweep only) and in solutions saturated with air in Figure 5. In all of the experiments, the first sweep showed greater reactivity and significant hysterisis between the negative and positive-going sweeps. This difference became negligible after about 10 sweeps. The curves shown all correspond to the first sweep in the negative-going direction.

The anodic reactivity of arsenopyrite increases with increasing sodium hydroxide concentrations in both

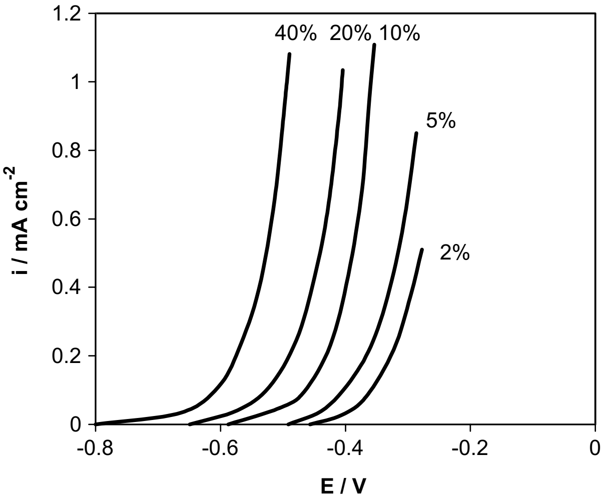

Fig. 4. Polarization curves of arsenopyrite in 40, 20, 10, 5 and 2% NaOH solutions in the absence of dissolved air.

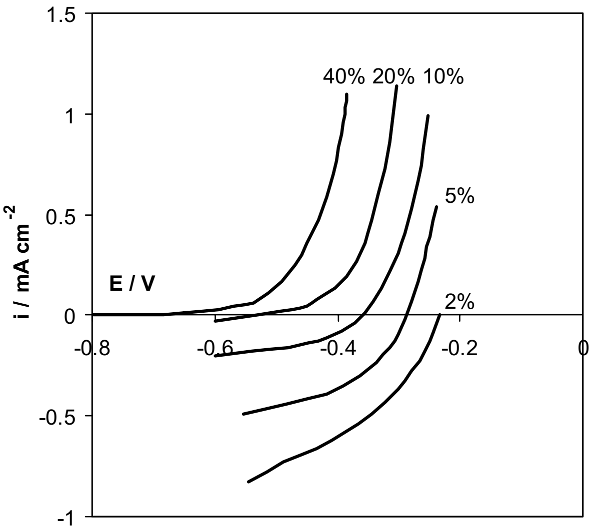

Fig. 5. Polarization curves of arsenopyrite in 40, 20, 10, 5 and 2% NaOH solutions in the presence of dissolved air.

cases. Oxidation of the arsenopyrite mineral surface was the only anodic process and no cathodic process was observed in the limited potential range studied in 40% NaOH solution both in the absence and presence of dissolved air. However, it was interesting to note that at the lower concentrations of sodium hydroxide a cathodic process started to occur within the experimental potential range. This cathodic process was observed in experiments performed in the presence of dissolved air and it was attributed to the reduction of oxygen in air saturated alkaline sodium hydroxide solution at the arsenopyrite electrode surface.

Similar experiments were also performed using more dilute solutions by bubbling pure oxygen into the solutions before and during the experiments to assess the effect of oxygen on the oxidation of arsenopyrite. The voltammograms obtained are shown in Figure 6.

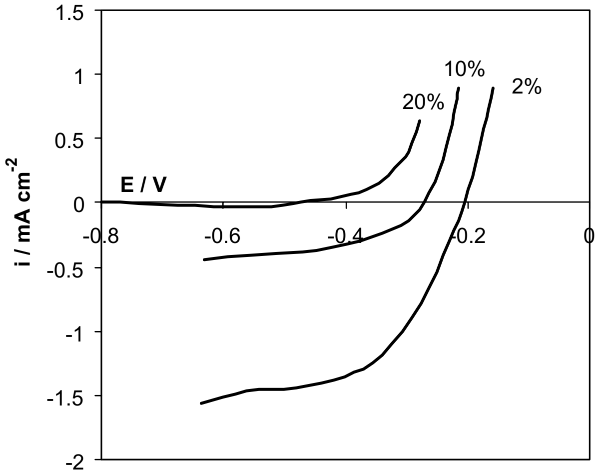

Fig. 6. Polarization curves of arsenopyrite in 20, 10, 5 and 2% NaOH solutions in the presence of dissolved oxygen.

As can be seen, the cathodic process is more obvious when oxygen is used instead of air and again its effect is more pronounced at lower concentrations of sodium hydroxide. The rate of reduction of oxygen at the arsenopyrite electrode surface in 2% sodium hydroxide solution for two different electrode rotation speeds was found to be proportional to the square root of the rotation speed of the electrode in the limiting current region.

The reduction of ferrate(VI) was also studied by recording voltammograms in deaerated solutions containing various concentrations of ferrate(VI) and the results of the first sweep in the negative direction from the rest potential obtained soon after immersing the electrode in the solution are shown in Figure 7. The shape of these curves suggest that the rate of reduction of ferrate(VI) at an arsenopyrite surface is controlled by mass transport at potentials in the region of the rest potential. The current plateau was found to be proportional to both the concentration of ferrate(VI) and the square root of the rotation speed of the electrode.

The effect of prolonged oxidation of the mineral on the cathodic reduction of ferrate(VI) was investigated by recording a voltammogram after increasing periods of open circuit in a ferrate(VI) solution. The results are shown in Figure 8 from which it is apparent that the rate of reduction of ferrate(VI) is significantly reduced by the accumulation of the product(s) of the oxidation of the mineral and/or the reduction of ferrate(VI).

3.3. *Potentiostatic current–time transients*

Electrochemical experiments were continued by recording the anodic current as a function of time for an arsenopyrite electrode in various NaOH solutions at potentials in the range of −500 to −300 mV in the absence of dissolved air. The curves obtained are given in Figure 9. The current decayed with time which was initially attributed to the formation of an oxide layer on the surface of the electrode. The electrode surface was

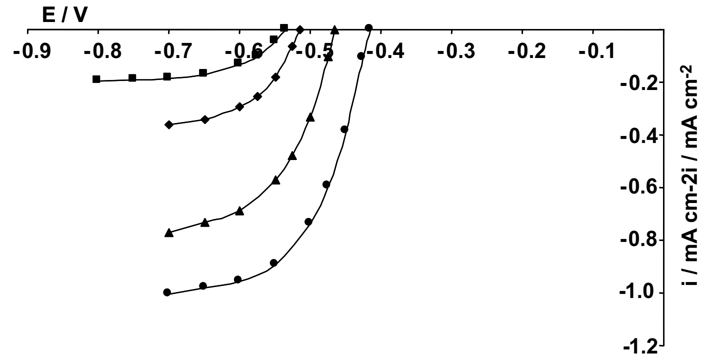

Fig. 7. Cathodic linear sweep voltammograms for the reduction of ferrate(VI) on an arsenopyrite rotating disc electrode in ferrate(VI) solutions of different concentrations: (♦) 3.16, (▲) 7.29, (●) 19.3 and (■) 1.48 mM.

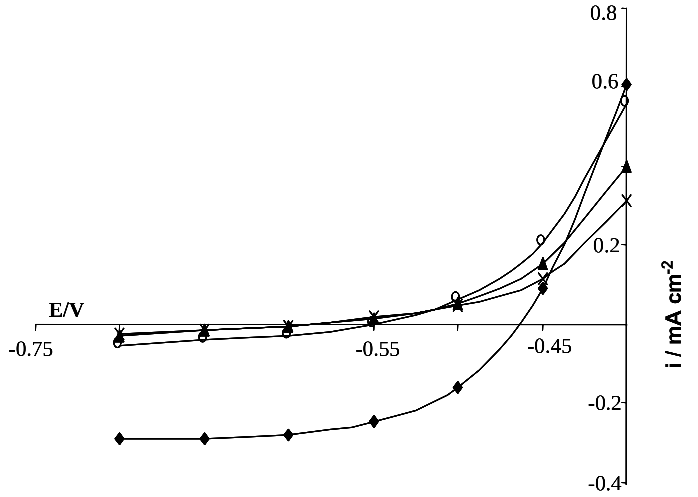

Fig. 8. Effect of prolonged oxidation of arsenopyrite on the cathodic reduction of ferrate(VI): Time: (♦) 10, (○) 20, (▲) 30 and (×) 40 min.

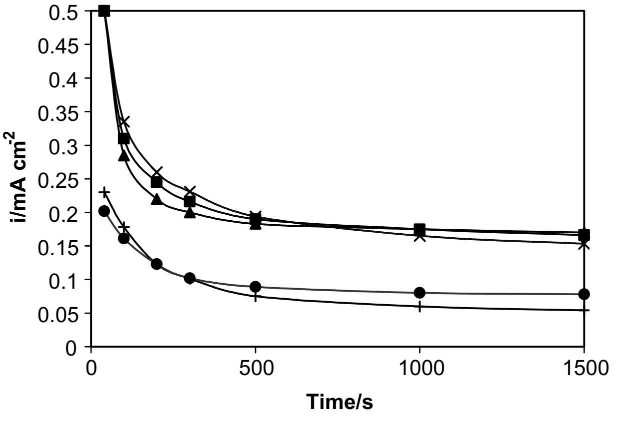

Fig. 9. Potentiostatic response of arsenopyrite in (×) 40, (■) 20, (▲)10, (●) 5 and (+) 2% NaOH solutions at potentials of −0.50 V, −0.44 V, −0.35 V, −0.30 V and −0.30 V, respectively.

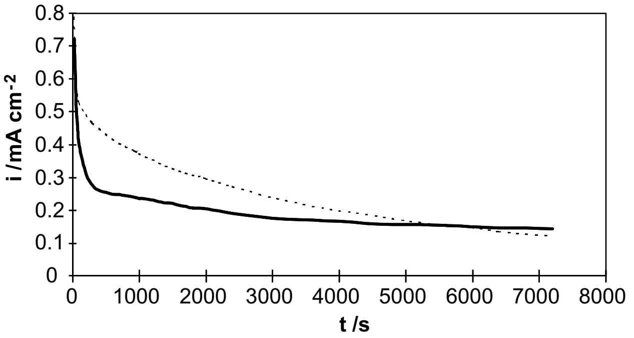

Fig. 10. Effect of rotation speed on the potentiostatic response of arsenopyrite in 40% NaOH solution at a fixed potential of −0.50 V. Speed: (—) 1000 rpm and (···) stationary.

investigated under optical microscope after the experiment performed in the 40% NaOH solution. It was not possible to visually detect any oxide layer on the surface. Therefore, the same experiment was repeated for a longer period of time, namely 2 h. In the first experiment, the electrode was rotated and again no change was observed on the surface by optical microscopy after the experiment. In the second experiment, the electrode was stationary and some brown and blue interference patterns were observed on the surface. The data obtained for these experiments are given in Figure 10. Surprisingly, the decay in current was more rapid when the electrode was rotated which could suggest the formation of a soluble intermediate product such as As(III) or Fe(II).

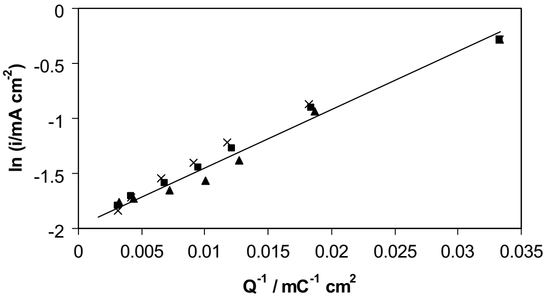

Fig. 11. Analysis of the potentiostatic current–time transients for the oxidation of arsenopyrite in (×) 40, (■) 20, and (▲) 5% NaOH solutions at potentials of −0.50 V, −0.44 V and −0.30 V, respectively.

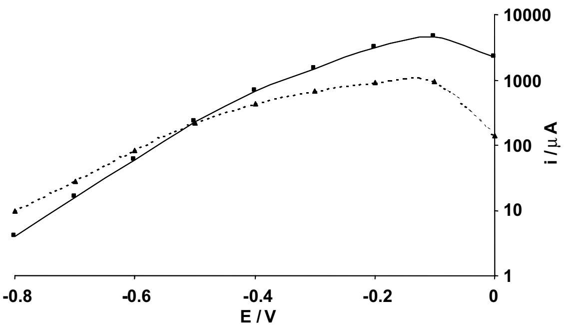

Fig. 12. Disc (■) and ring (×20) (···▲···) currents during the anodic oxidation of arsenopyrite in a deaerated 40% sodium hydroxide solution. Ring potential 0.5 V vs SCE.

3.4. *Ring-disc electrode experiments*

The unusual increase in the anodic current with decreasing agitation suggested that As(III) could be an intermediate product in the oxidation and several experiments were conducted with the ring-disc electrode to explore this possibility. Independent experiments with a rotating platinum disc electrode showed that, at potentials of 0.5 V and above, oxidation of As(III) to As(V) is mass-transport controlled in 40% sodium hydroxide solutions. The ring was therefore held at this potential while the disc potential was swept anodically from the rest potential in a deaerated sodium hydroxide solution. The resulting disc and ring currents are shown in Figure 11. The response of the ring during a potentiostatic current-time transient on the disc is shown in Figure 12.

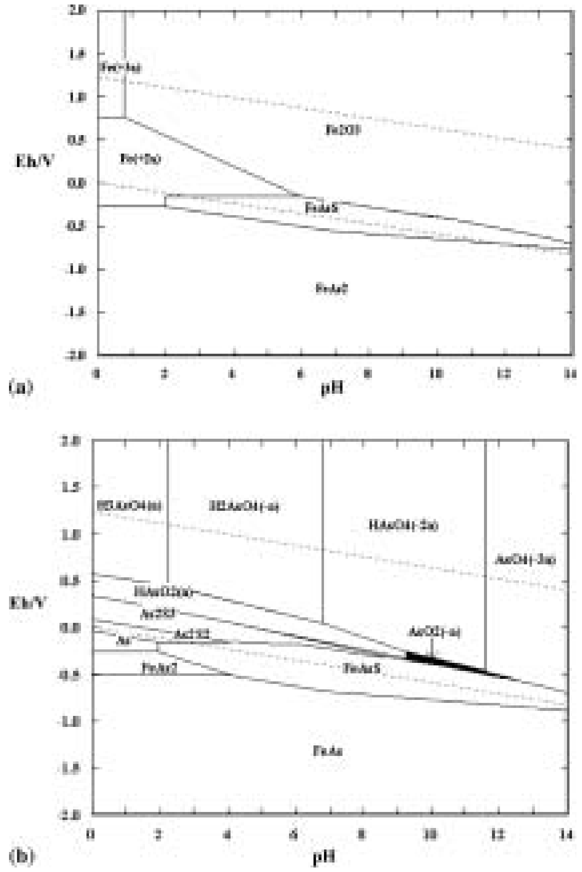

Fig. 13. (a) Eh–pH diagram for arsenopyrite showing the iron species. Activity of soluble species is 10^{-3} M [13]. (b) Eh–pH diagram for arsenopyrite showing the arsenic species. Activity of soluble species is 10^{-3} M [13].

4. Discussion

The Eh–pH diagram for the Fe–As–S system [11] for 10^{-3} M dissolved species is shown in Figure 13(a) and (b). The rest potentials measured in the presence of ferrate(VI) or in the presence of oxygen all fall within the region of stability of ferric hydroxide, the arsenate ion and the sulfate ion. On this basis, the following reaction is thermodynamically favoured for the oxidation of arsenopyrite in alkaline solutions:

$$\mathrm{FeAsS} + 19\mathrm{OH}^- \rightarrow \mathrm{Fe(OH)_3} + \mathrm{AsO_4^{3-}} + \mathrm{SO_4^{2-}} + 8\mathrm{H_2O} + 14\mathrm{e}^- \qquad (6)$$

according to this reaction, oxidation of arsenopyrite is a 14 electron transfer process and arsenic dissolves as arsenate, As(V). This reaction has generally been assumed by previous investigators of the anodic behaviour of arsenopyrite.

The rest potential of arsenopyrite in the presence of ferrate(VI) exhibits different behaviour depending on the concentration of ferrate(VI) in 40% NaOH solution as shown in Figure 2. Thus, at high concentrations, the potential decreases with time and becomes increasingly less dependent on the rotation speed of the electrode. On the other hand, at low concentrations, the potential attains a steady value with retention of the dependence on the rotation speed over a period of at least one hour. This difference in behaviour can be attributed to the relative rates of formation of partially passivating surface layers containing iron hydroxides produced by both anodic oxidation of the mineral and cathodic reduction of ferrate(VI). At low ferrate(VI) concentrations, it appears as if the precipitation may be occurring away from the electrode surface. Assuming that the process is controlled by mass transport of ferrate(VI) to the electrode surface at low concentrations, and that the process occurs in the Tafel region for the anodic dissolution of arsenopyrite, a Tafel slope can be estimated as 100 mV decade^{-1} from the dependence of the mixed potential on the rotation speed of the electrode. This is somewhat different from values of from 200 to 230 mV decade^{-1} that can be obtained from Tafel plots of the anodic oxidation data shown in Figure 4. This latter value is similar to that found for the oxidation of pyrite in ferrate solutions in a previous study [9], namely 223 mV decade^{-1}.

The rest potential in oxygenated solutions in the absence of ferrate(VI) shows similar behaviour as shown by the data in Figure 3. It is apparent that the effect of agitation is less pronounced with oxygen as the oxidant, especially at lower concentrations of sodium hydroxide. The rate of oxidation under these conditions is thus only partially controlled by mass transport to the mineral surface. The positive shift of the potential with decreasing alkalinity is consistent with the positive shift of the anodic oxidation reaction in the same direction as shown in Figure 4.

The anodic characteristics of the mineral are very similar to those of pyrite [9] in strongly alkaline solutions, that is, smoothly increasing oxidation with a Tafel slope of about 220 mV decade^{-1} in the region of the rest potentials measured above. The negative shift with increasing alkalinity is not unexpected given the overall pH dependence of the reaction. It is not possible to derive a reaction order with respect to the hydroxyl ion given the variations in ionic activities in the concentrated solutions but it appears to be greater than first order. It appears that the rate determining step in the anodic oxidation therefore involves transfer of a single electron with one or more hydroxyl ions also involved. Given the complex overall reaction, it would be highly speculative to suggest a mechanism at this stage.

The electrochemical behaviour in aerated (Figure 5) and oxygenated (Figure 6) solutions shows an unexpected trend with increasing alkalinity in that the reduction of oxygen becomes strongly inhibited in the more concentrated solutions. Thus, in the most dilute (2% NaOH) solution, the reduction of oxygen is mass transport controlled at potentials within 100 mV of the rest potential while there is no obvious reduction in the more concentrated (20%, 40%) solutions within the potential range studied. The limiting current for reduction in the 2% solution was found to be approximately proportional to the square root of the rotation speed and was calculated as 2.8 mA cm^{-2} for a four-electron process at 1000 rpm using the Levich equation and recent data on the solubility and diffusivity of oxygen in caustic soda solutions [12]. This compares with that measured of 1.45 mA cm^{-2}. The indication of two cathodic waves in the cathodic sweep in the 2% NaOH solution and the above ratio of about 2 suggests that reduction of oxygen to peroxide may precede reduction to water. This effect of the alkalinity on the reduction of oxygen has significant implications in any process options which will utilize alkaline oxidation of the mineral.

The characteristics of the cathodic reduction of ferrate(VI) in 40% NaOH solution are shown in Figure 7 from which it is apparent that the initial reduction process is mass transport controlled at the rest potentials of the mineral in such solutions. However, as found from the dependence of the rest potential on the rotation speed, prolonged oxidation particularly at high ferrate(VI) concentrations, results in reduced rates of reaction. This is illustrated by the results in Figure 8 which shows that oxidation of the mineral by ferrate(VI) results in decreasing activity for the reduction of ferrate(VI) due to the formation of a passivating layer which is not reduced in the potential region studied.

The formation of this passive layer is reflected in the current–time transients shown in Figure 9. The form of these transients and the charge involved is typical of the growth of a thick, partially passivating layer produced by a dissolution–precipitation process. This is suggested by the linearity of the Mott–Cabrera plots [15] shown in Figure 10 in which Q is the total charge passed. The unusual observation shown in Figure 11 in which the current is higher at a stationary electrode than a rotating electrode suggested that a soluble intermediate such as arsenic(III) or iron(II) was formed which was more rapidly transported from the electrode in the case of the rotating electrode. With this in mind, preliminary experiments with a rotating arsenopyrite disc/platinum ring electrode revealed that this was indeed the case as shown by the data in Figure 12.

Thus, for the following reactions on the disc and ring,

$$\text{Disc: } \mathrm{FeAsS} + 17\mathrm{OH}^- \rightarrow \mathrm{Fe(OH)}_3 + \mathrm{AsO}_3^{3-} + \mathrm{SO}_4^{2-} + 7\mathrm{H}_2\mathrm{O} + 12\mathrm{e}^-$$

$$\text{Ring: } \mathrm{AsO}_3^{3-} + 2\mathrm{OH}^- = \mathrm{AsO}_4^{3-} + \mathrm{H}_2\mathrm{O} + 2\mathrm{e}^-$$

the apparent collection efficiency is $N/6 = 0.05$ where N $(= 0.30)$ is the geometric or true collection efficiency. This is consistent with the data in Figure 12 which shows that the ring current is approximately 1/20th of the disc current at potentials below about −0.4 V. At higher potentials, the apparent collection efficiency decreases with increasing potential as an increasing proportion of the arsenic(III) is oxidized to arsenic(IV) on the disc. In this regard, it is possible that the broad peak above −0.2 V could be due to the precipitation of ferric arsenate on the electrode.

5. Conclusions

The anodic oxidation of arsenopyrite in alkaline solutions has been found to be a complex process with the initial formation of arsenic(III), iron(III) and sulfate as the products of oxidation. Partial passivation of the process is caused by the precipitation of a layer of amorphous ferric hydroxide on the surface of the mineral. This layer also reduces the rate of reduction of dissolved oxygen and the ferrate(VI) ion at the surface. The initial rates of reduction of both these species are mass transport controlled at potentials close to the mixed potential of the mineral in alkaline solutions containing these species.

Acknowledgements

The authors would like to thank the A.J. Parker Cooperative Research Centre for Hydrometallurgy and The Scientific and Technical Research Council of Turkey (TUBITAK) for the financial support provided throughout this study.

References

1. C. Gasparrini, *CIM Bulletin* **76** (851) (1983) 144–153.
2. N.J. Cook and S.L. Chryssoulis, *Can. Mineral.* **28** (1990) 1.
3. G.M. Kostina and A.S. Chernyak, *Zh. Prikl. Khim.* **49** (1976) 1534.
4. M.J.V. Beattie and G.W. Poling, *Int. J. Min. Process.* **20** (1987) 87.
5. G.K. Sisenov, V.A. Bogdanovskaya and M.R. Tarasevich, *Soviet Electrochem.* **24**(6) (1988) 729.
6. V.M. Sanchez, and J.B. Hiskey, *Miner. Metall. Process.* **8** (1991) 1.
7. X.-H. Wang, E. Ahlberg and K.S.E. Forsberg, *J. Appl. Electrochem.* **22** (1992) 1095.
8. P. Bakta, J.W. Langhans and K.P.V. Lei, US Department of the Interior, 'Bureau of Mines, Report No 9258' (1989).
9. N. De Jager and M.J. Nicol, International Symposium on 'Electrometallurgy', 2000 SME Annual Meeting and Exhibition, Florida, EPD 1997 (Littleton, CO 1997).
10. J.M. Schreyer, G.W. Thompson and L.T. Ockerman, *Anal. Chem.* **22** (1950) 1426.
11. 'HSC Chemistry', Ver. 4.1, Outokumpu Research Oy, Pori, Finland (1974–99).
12. M. Chatenet, M. Aurousseau and R. Durand, *Electrochim. Acta* **45** (2000) 2823.
13. M.J. Dignam, *Can. J. Chem.* **42** (1964) 1155.